

## Experimental study on the minimum design metal temperature of Q345R steel\*

Xiang-yu SHU<sup>1</sup>, Ying-zhe WU<sup>1</sup>, Jin-yang ZHENG<sup>†‡1</sup>, Bi-nan SHOU<sup>2</sup>

<sup>1</sup>Institute of Process Equipment, Zhejiang University, Hangzhou 310027, China

<sup>2</sup>National Technology Research Center on Pressure Vessel and Pipeline Safety Engineering, Hefei 215021, China

<sup>†</sup>E-mail: jyzh@zju.edu.cn

Received Apr. 10, 2017; Revision accepted Nov. 24, 2017; Crosschecked June 6, 2018

**Abstract:** As the material most widely used in manufacturing pressure vessels in China, Q345R steel has been permitted in ASME Code Case 2642 to be used for fabricating pressure vessels since 2010. It is listed in the material group corresponding to the exemption curve A for Charpy V-notched (CVN) impact test requirements. However, recent studies indicate that the mechanical property of Q345R has been underestimated and the curve A classification is over-conservative. In this paper, the  $K_{Ic}-T$  relationship for two batches of Q345R produced in 2009 and 2014 is empirically obtained by curve-fitting and regression analysis from a large amount of CVN data based on  $K_{Ic}$ -CVN correlations and the temperature-shift method. Based on the theory of derivation for the ASME exemption curves, the specific exemption curves for the two batches are generated by combining the  $K_{Ic}-T$  relationship and the  $K_{I(\min)}-t$  relationship developed from the failure assessment diagram (FAD). Such exemption curve is not in parallel to the ASME curves, and lies over curve C and between curves B and D, but better reflects the actual toughness and expands the impact test exemption area, especially for small components with a thickness less than 20 mm. Furthermore, the method presented in this paper (the Materials Properties Council (MPC) method) is compared with the master curve (MC) method, concluding that the two methods are reliable for determining the exemption curve, and the MC method expands a further area for the impact test exemption and results in a lower minimum design metal temperature (MDMT) than the MPC method.

**Key words:** Q345R steel; Exemption curve; Master curve (MC); Charpy V-notched impact test; Fracture toughness  
<https://doi.org/10.1631/jzus.A1700188>

**CLC number:** TH142.1; TH140.7

### 1 Introduction

For pressure vessel steel with body center cubic (BCC) lattices, such as Chinese Q345R steel, a cleavage fracture (brittle fracture) would probably occur without any large deformation as the temperature drops into the brittle region, possibly causing a severe accident. To avoid such a tragedy, during the past few decades, several testing methods for estimating fracture toughness have been developed and

widely used. Among these, Charpy V-notched (CVN) impact test is the method most commonly used in surveillance procedures because it requires only small and cheap specimens that have simple geometry and can be easily prepared.

Based on linear elastic fracture mechanics, the exemption curve method has been developed as a new surveillance procedure in ASME BPVC VIII-1 and VIII-2 (ASME, 2015a, 2015b). The latest version of the exemption curves was issued in ASME BPVC VIII-2 in 2007 (Fig. 1). If served below the minimum design metal temperature (MDMT) provided by exemption curves, material must meet the CVN requirements without regard to the lower shelf operation nor other specified conditions. Classified by four different reference temperatures, the exemption

<sup>‡</sup> Corresponding author

\* Project supported by the National Key Research and Development Program of China (No.2016YFC0801905).

 ORCID: Xiang-yu SHU, <https://orcid.org/0000-0001-7591-8332>

© Zhejiang University and Springer-Verlag GmbH Germany, part of Springer Nature 2018

curves comprise four different curves labeled A, B, C, and D, respectively. Material under consideration is also classified into four groups corresponding to the four curves.

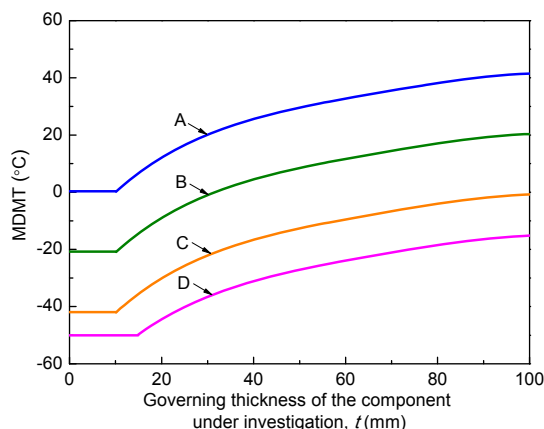


Fig. 1 Exemption curves in ASME BPVC VIII-2

With the implementation of Chinese standard GB/T 713 (SAC, 2014) in 2008, Q345R is the material most widely used in manufacturing boilers and vessels in China because of its excellent mechanical performance. It has also been permitted in ASME Code Case 2642 (ASME, 2010) for use in pressure vessels since 2010. However, it is listed in the group corresponding to exemption curve A with respect to CVN requirements. Thus, Q345R can be used only above  $-10\text{ }^{\circ}\text{C}$  without regard to the lower shelf operation. Relevant studies (Cao et al., 2008; Shu et al., 2013; Cui et al., 2015; Gui et al., 2016) in recent years indicate that the toughness of Q345R is underestimated by classifying it into exemption curve A. Cui et al. (2015) discussed the applicability of the exemption curve to Q345R steel, and concluded that Q345R can be used safely at the MDMT of exemption curve D based on a series of mechanical tests and the fracture toughness given by the master curve (MC) method. However, the influence of the loading rate was not considered. Furthermore, there was no specific exemption curve for Q345R steel. A specific exemption curve is attractive as it can instruct the verification of the material in relation to toughness requirements and enable its more economical use. In this study, specified exemption curves for Q345R steel produced in 2009 (using the MPC method de-

veloped from the model suggested by the Materials Properties Council) and 2014 (using the MPC and MC methods) were developed taking into account the loading rate. Such exemption curves expand the impact test exemption area, especially for components with small thickness. A comparison made between the MPC method and the MC method in derivation of exemption curves showed that both of the two methods are reliable for determining the exemption curve, and the MC method expands a further area for the impact test exemption and results in a lower MDMT than the MPC method.

First, the tensile tests, CVN tests, quasi-static fracture toughness tests for the MC method, and the MC for Q345R steel are presented. Then, the Sailors–Corten correlation is used to determine the empirical relationship between CVN energies and quasi-static fracture toughness data as it has been proved to be more accurate for Q345R steel. The derivation of the specific exemption curve for Q345R steel using the MPC method is analyzed, based on which the specific exemption curve for Q345R is obtained. The difference between the specific exemption curve for Q345R steel and the ASME exemption curves is discussed. Furthermore, the development of a specific exemption curve by using the MC method is presented, and the results are compared with those from the MPC method.

## 2 Material and experimental data

### 2.1 Material

In this study, a large amount of CVN data from previous study (Shu et al., 2013) was used, so that statistically reliable results could be obtained. Those data were gathered from Q345R steel produced in 2009 (Q345R-2009 for short). However, recent studies (Cao et al., 2008; Shu et al., 2013; Cui et al., 2015; Gui et al., 2016) show that the fracture toughness performance of Q345R has improved in recent years, thanks to the development of metallurgy and equipment in China. Nevertheless, those conservative data (Shu et al., 2013) are still valid and therefore were used in this study.

We used three Q345R steel plates, each with a thickness of 28 mm, produced in 2014 (Q345R-2014

for short) to study the toughness property using the MC method. The plates were made by one of the same manufacturers and their chemical composition (Table 1) met the requirements specified by the same Chinese standard GB/T 713 (SAC, 2014) as in the previous study (Shu et al., 2013).

**Table 1 Chemical composition of Q345R steel plates provided in 2014 (% in weight)**

Plate No.	Chemical composition (%)				
	C	Si	Mn	P	S
01	0.15	0.37	1.40	0.014	0.004
02	0.15	0.38	1.45	0.018	0.004
03	0.15	0.38	1.39	0.010	0.003

## 2.2 Experimental data

### 2.2.1 Tensile test

In addition to the previous study (Shu et al., 2013), 10 tensile tests for the same Q345R-2009 were carried out at ambient temperature to evaluate the yield strength, which is an essential input for calculating the fracture toughness,  $K_{Ic}$ , from the upper shelf CVN data (Section 3.2.1). All the tensile test specimens in the present study were standard round bars with a diameter of 5 mm for the parallel length, and the axis of the sample was along the longitudinal direction of the plate. The yield strength for Q345R-2009 was conservatively chosen to be 351 MPa, which was the minimum value from 10 tests at ambient temperature.

Another 15 tensile tests of Q345R-2014 (five tests for each plate) were conducted at from  $-50\text{ }^{\circ}\text{C}$  to  $-150\text{ }^{\circ}\text{C}$  to evaluate yield and ultimate tensile strength at sub-zero temperatures for the MC method. Liquid nitrogen and a cryo-chamber were used for the low temperature testing environments. The result at each temperature is shown in Fig. 2. Eq. (1) shows the expression for the fitting curve for yield strength  $\sigma_{ys}$ :

$$\sigma_{ys}(T) = 410.4 - 0.2T + 0.01T^2 - 2.9 \times 10^{-7}T^3. \quad (1)$$

Three tensile tests (one for each plate) at ambient temperature were carried out. The minimum tensile yield strength from the three tests was 408 MPa.

### 2.2.2 Charpy V-notched impact tests

The CVN data of Q345R-2009 were taken from Shu et al. (2013). To determine the quasi-static fracture toughness test temperature of the MC method for Q345-2014, the CVN tests were carried out at variety of temperatures from  $-196\text{ }^{\circ}\text{C}$  to  $20\text{ }^{\circ}\text{C}$  (Fig. 3), using a pendulum impact tester with a temperature control system and specimen auto-delivery system. For each steel plate, 18 standard full-size CVN specimens were prepared as T-L specimens, of which the notch plane was perpendicular to the long transverse orientation of the plate, and the crack grew parallel to the longitudinal orientation. In accordance with GB/T 2975 (SAC, 1998) and GB/T 713 (SAC, 2014), which are equivalent to ISO 377 and ISO 9328-2, respectively, test specimens were taken at a position 2 mm away from the surface of the steel plane since the thickness was not over 40 mm.

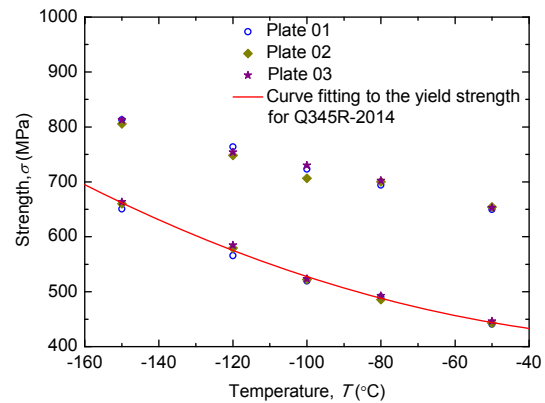


**Fig. 2 Tensile tests: yield and ultimate tensile strength for Q345R-2014 at sub-zero temperatures and curve fitting for the yield strength**

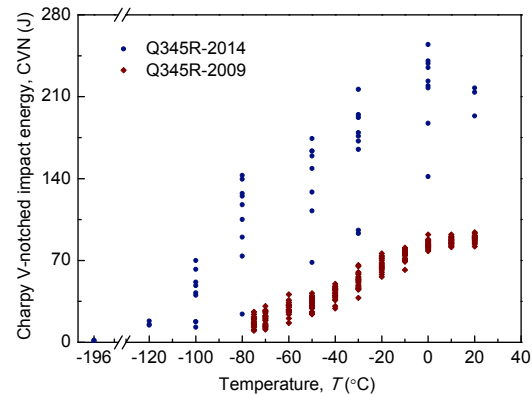


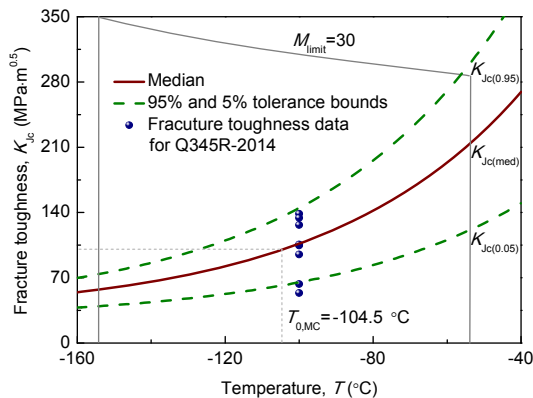
**Fig. 3 Charpy V-notched impact tests: CVN data for Q345R-2009 (Shu et al., 2013) and Q345R-2014**

### 2.2.3 Fracture toughness tests

Nine standard compact tension specimens (1T-C(T)) of Q345R-2014 (three specimens for each plate) in T-L orientation, each with a thickness of 25.4 mm (represented as 1T), were prepared in accordance with ASTM E399 (ASTM, 2012). The 1T-C(T) specimens were fatigue pre-cracked to introduce a sharp crack tip at ambient temperature with a minimum pre-crack length of more than 2 mm in accordance with ASTM E1921 (ASTM, 2016). Fracture toughness tests were carried out according to ASTM E1921 at a test temperature of  $-100\text{ }^{\circ}\text{C}$ , which was estimated from CVN data beforehand (Section 3.2.1). Finally, the fracture toughness data of eight 1T-C(T) specimens consisting of three from Plate 01, two from Plate 02, and three from Plate 03 were calculated to be valid, and all these data were sufficient to draw the MC for Q345R-2014. The experimental setup is shown in Fig. 4a, and the fracture toughness data and the MC curve in Fig. 4b, where  $K_{Jc}$  is the



(a)



(b)

**Fig. 4 Quasi-static fracture toughness test (C(T))**  
(a) Experimental setup; (b) Fracture toughness data and master curve for Q345R-2014

quasi-static fracture toughness  $K_{Jc}$  calculated from J-integral in the MC method,  $M_{limit}$  represents the deformation of the specimen during the test,  $K_{Jc(med)}$  is the median  $K_{Jc}$  for the Weibull distribution,  $K_{Jc(0.95)}$  and  $K_{Jc(0.05)}$  represent the 95% and 5% tolerance bounds for  $K_{Jc}$ , respectively, and  $T_{0,MC}$  is the reference temperature at which  $K_{Jc(med)}$  equals  $100\text{ MPa}\sqrt{\text{m}}$ .

Data from quasi-static fracture toughness tests with standard 25.4 mm thick SE(B) specimens conducted by other studies (Cao et al., 2008; Cui et al., 2015; Gui et al., 2016) were taken and are shown in Fig. 6. The data were applied to determine the most appropriate empirical correlation between the CVN energy and the quasi-static fracture toughness for Q345R steel (Section 3.2.1).

## 3 Exemption curves for Q345R

To derive the exemption curves for Q345R, two essential inputs are required: the relationship between the minimum required fracture toughness ( $K_{I(min)}$ ) and the thickness of the component ( $t$ ), and the fracture toughness of Q345R ( $K_c$ ) as a function of the temperature ( $T$ ). In this section, the test data for Q345R-2009 are discussed.

### 3.1 $K_{I(min)}$ - $t$ relationship

$K_{I(min)}$ - $t$  relationship describes the minimum required fracture toughness of the material for a given component thickness. The failure assessment diagram (FAD) method described in API 579-1/ASME FFS-1 (ASME, 2007) was used. The FAD approach provides a technical-based, convenient method to determine whether an in-service component with a crack-like flaw is acceptable. In this method, the driving force for the failure is measured by two distinct criteria: the unstable fracture that controls the brittle failure and the limit load that, by causing plastic collapse, controls the ductile fracture. A mixed mode fracture occurs between these extremes (ASME, 2007; Prager et al., 2010). For such evaluation, the component structure, reference flaw size, loadings on the component, and material strength are required parameters.

#### 3.1.1 Reference component

As a typical component of pressure vessels, a

cylinder with a thickness of  $t$  and a radius to thickness ratio  $R/t$  was assumed for reference.

### 3.1.2 Reference flaw

Buried flaws are more likely to escape detection than surface flaws, but when not too near the surface produce only about half the stress intensity factor value for a given size. Therefore, located on the surface, a semi-elliptical flaw in the longitudinal direction, perpendicular to the direction of maximum stress, with a depth of  $a$  and a length of  $2c$  was assumed in the cylinder, where  $a$  and  $2c$  are determined by

$$a = \min \left[ \frac{t}{4}, 25.4 \text{ mm} \right], \quad (2)$$

$$2c = 6a. \quad (3)$$

The flaw size given by Eqs. (2) and (3) was based on the sensitivity and the detection capability of non-destructive testing technology in early years (PVRC, 1972), and is quite conservative for today.

### 3.1.3 Stress condition

The maximum allowable primary stress  $\sigma_m^P$  and residual stress  $\sigma_m^{SR}$  are used for calculating the driving force of the flaw (Prager et al., 2010). With a common conservative approximation, the stresses are assumed based on the allowable stresses of materials in design progress for pressure vessels. Thus,  $\sigma_m^P$  was evaluated as

$$\sigma_m^P = \sigma_{ys} / 1.5, \quad (4)$$

while  $\sigma_m^{SR}$  was calculated based on Eq. (5) for the as-welded condition (AW) and Eq. (6) for the post-weld heat treatment or non-welded condition (PWHT/NW).

$$\sigma_m^{SR} = 0.2\sigma_{ys}, \quad \text{for AW}, \quad (5)$$

$$\sigma_m^{SR} = \sigma_{ys} / 1.5, \quad \text{for PWHT/NW}, \quad (6)$$

where  $\sigma_{ys}$  is the engineering yield stress evaluated at the temperature of interest. Conservatively, for

Q345R,  $\sigma_{ys}$  was set to be 351 MPa, the yield strength measured at the ambient temperature (Section 2.2.1).

### 3.1.4 Failure assessment diagram

The FAD approach is usually used for evaluating the acceptability of crack-like flaws with a known fracture toughness of the material. However, we used the FAD method inversely to determine a critical (minimum) required fracture toughness  $K_{I(\min)}$  of the material based on given reference flaws and stress conditions.

One typical form of the FAD curve (ASME, 2007) represents a maximum allowable toughness ratio  $K_{r(\max)}$  at a given load ratio of primary stress  $L_r^P$ , which can be approximately calculated by

$$K_{r(\max)} = [1.0 - (L_r^P)^{2.5}]^{0.2}. \quad (7)$$

Eq. (7) stands only if the steel has a yield point plateau as has Q345R. In this case, the maximum permitted load ratio based on the primary stress  $L_{r(\max)}^P$  equals one. Therefore,  $K_{I(\min)}$  can be given by the definition of the fracture toughness ratio according to API 579-1/ASME FFS-1:

$$K_{I(\min)} = \frac{K_1^P + \Phi K_1^{SR}}{K_{r(\max)}} = \frac{K_1^P + \Phi(L_r^P, L_r^{SR})K_1^{SR}}{[1.0 - (L_r^P)^{2.5}]^{0.2}}, \quad (8)$$

where  $K_1^P$  and  $K_1^{SR}$  are the stress intensity factors based on the primary stresses and secondary/residual stresses, respectively.  $\Phi$  is a plasticity correction factor that is derived by curve fitting and presented as a function of  $L_r^P$  and  $L_r^{SR}$  (load ratio based on the secondary/residual stresses). All variables,  $K_1^P$ ,  $K_1^{SR}$ ,  $L_r^P$ , and  $L_r^{SR}$ , can be calculated by WRC 528 (Prager et al., 2010):

$$K_1^P = \sigma_m^P K_{RF}^{Cylinder}(t, R/t), \quad (9)$$

$$K_1^{SR} = \sigma_m^{SR} K_{RF}^{Cylinder}(t, R/t), \quad (10)$$

$$L_r^P = \frac{\sigma_m^P}{\sigma_{ys}} R_{RF}^{Cylinder}(t, R/t), \quad (11)$$

$$L_r^{SR} = \frac{\sigma_m^{SR}}{\sigma_{ys}} R_{RF}^{Cylinder}(t, R/t), \quad (12)$$

where  $K_{RF}^{Cylinder}$  is the reference parameter of the stress intensity factor, and  $R_{RF}^{Cylinder}$  is the reference parameter of stress. They were derived by using the KCSCLE2 solution and RCSCLE2 solution in API 579, respectively, with the given reference flaw (Section 3.1.2) and a specified unit of membrane stress, and are presented as a function of  $t$  and the radius-to-thickness ratio  $R/t$ . In this study, the value of  $R/t$  was set to 100 because the toughness ratio  $K_r$  rises slowly when  $R/t$  is over 100 (Cui et al., 2015).

Given a constant ratio of stresses to the yield strength (Section 3.1.3), the  $K_{I(min)}-t$  relationship can be obtained (Fig. 5).

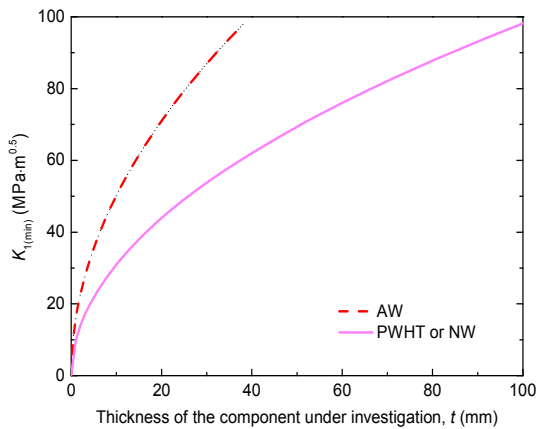


**Fig. 5** Minimum required fracture toughness as a function of the component thickness with  $\sigma_{ys}$  of 351 MPa, based on as-welded (AW) conditions and post-weld heat treatment (PWHT) or non-welded (NW) conditions

### 3.2 $K_c-T$ relationship

The relationship between the fracture toughness  $K_c$  of the material and the temperature  $T$  was empirically obtained from extensive CVN testing at a variety of temperatures.

#### 3.2.1 Converting CVN to $K_{Ic}$

As suggested in API 579-1/ASME FFS-1, the Rolfe–Novak–Barsom correlation (Barsom and Rolfe, 1970; Rolfe and Novak, 1970; Roberts and Newton, 1981; ASME, 2007),

$$\left(\frac{K_{Ic,us}}{\sigma_{ys}}\right)^2 = 0.64 \left(\frac{CVN_{us}}{\sigma_{ys}} - 0.01\right), \quad (13)$$

was used to correlate the quasi-static fracture toughness  $K_{Ic}$  and measured CVN energies for the upper shelf region (subscript “us” represents the upper shelf region), while the Sailors–Corten correlation (Sailors and Corten, 1971; Roberts and Newton, 1981; ASME, 2007; Prager et al., 2010),

$$K_{Ic,tl} = 14.6\sqrt{CVN_{tl}}, \quad (14)$$

was selected for the transition and the lower shelf regions (subscript “tl” represents the transition and the lower shelf regions).

Several correlations for the transition region were proposed in early studies (Barsom and Rolfe, 1970; Sailors and Corten, 1971; Thorby and Ferguson, 1976; BSI, 2005). To determine which is the most suitable  $K_{Ic}$ –CVN correlation for Q345R in the transition region,  $K_{Ic}$ –CVN data were collected from recent literature (Cao et al., 2008; Cui et al., 2015; Gui et al., 2016). Fig. 6 shows that Eq. (14) for the Sailors–Corten correlation fits the  $K_{Ic}$ –CVN data best within the entire range of CVN energies.

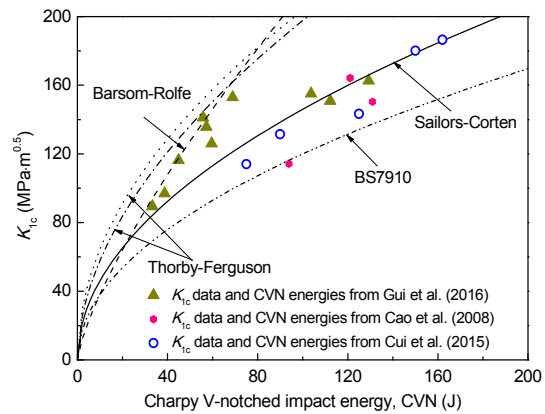


**Fig. 6** Experimental  $K_{Ic}$ –CVN data and curves for various correlations for Q345R in the transition region

Furthermore, to determine the test temperature  $T_{MC}$  for the MC of Q345R-2014, an estimation procedure was provided in ASTM E1921. For 1T-C(T) specimens,  $T_{MC}$  can be determined by

$$T_{MC} = T_{28J} - 18, \quad (15)$$

$$T_{MC} = T_{41J} - 24, \quad (16)$$

where  $T_{28J}$  and  $T_{41J}$  refer to the CVN test temperatures where the energies equal 28 J and 41 J, respectively. By using the hyperbolic tangent function, the CVN data for Q345R-2014 were fitted along with 95% prediction bands (Fig. 7).

The expression of the fitting curve is shown in Eq. (17), where  $T_{28J}$  and  $T_{41J}$  equal  $-124.23\text{ }^{\circ}\text{C}$  and  $-106.75\text{ }^{\circ}\text{C}$ , respectively. Thus,  $T_{MC}$  is calculated to be  $-142.23\text{ }^{\circ}\text{C}$  (for  $T_{28J}$ ) or  $-148.23\text{ }^{\circ}\text{C}$  (for  $T_{41J}$ ).

$$CVN_{2014} = 119.94 + 118.48 \tanh\left(\frac{T + 59.23}{62.79}\right). \quad (17)$$

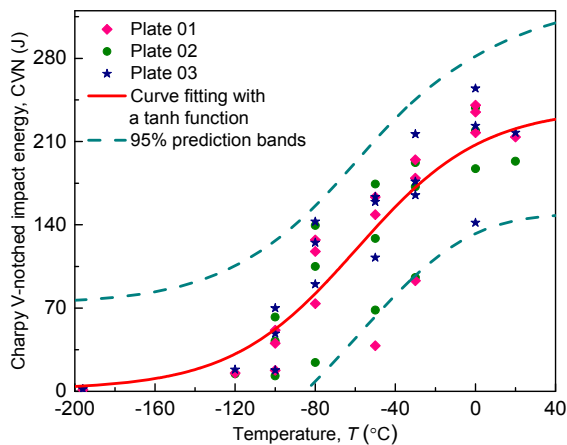


Fig. 7 Concatenated hyperbolic tangent fitting with 95% prediction bands of CVN energies for Q345R-2014

$T_{MC}$  actually is the predicted temperature at which the fracture toughness of the C(T) test should equal or be close to  $100\text{ MPa}\sqrt{\text{m}}$ . By using the Sailors–Corten correlation, the CVN energy equals 46.91 J when the fracture toughness is  $100\text{ MPa}\sqrt{\text{m}}$ . Thus,  $T_{MC}$  can be the test temperature at which the CVN energy is 46.91 J. Thus, the  $T_{MC}$  was calculated to be  $-98.82\text{ }^{\circ}\text{C}$ , which is much lower than the  $T_{MC}$  calculated from Eqs. (15) and (16). Then, the fracture toughness tests in Section 2.2.3 were carried out at  $-100\text{ }^{\circ}\text{C}$ . Finally, the reference temperature  $T_{0,MC}$ , where the fracture toughness equals  $100\text{ MPa}\sqrt{\text{m}}$  for the MC method, was calculated to be  $-104.52\text{ }^{\circ}\text{C}$ . Therefore, using the Sailors–Corten correlation proved to be more accurate and suitable for Q345R than Eqs. (15) and (16).

Thus, by using the Rolfe–Novak–Barsom correlation and the Sailors–Corten correlation, the CVN

data shown in Fig. 3 were then converted into the  $K_{Ic}$ – $T$  relationship with  $20\text{ }^{\circ}\text{C}$  for the upper shelf region and the other temperatures for the transition and lower shelf region (Fig. 8).

### 3.2.2 Dynamic fracture toughness

Low alloy steels, such as Q345R, are very sensitive to the loading rate (strain rate). The toughness of such material drops rapidly as the loading rate increases. Therefore, it is more accurate to consider the dynamic fracture toughness  $K_{I_d}$  with the corresponding loading rate of the components under the investigation to evaluate the suitability of the material. In normal operation, for most pressure vessels, the pressure stress and the thermal stress change very slowly. However, from a reliability and safety point of view, accident conditions such as water hammer, earthquakes with a relatively low loading rate, bullet or missile penetration incidents, and “crack pop-in” from the brittle region with a very high loading rate are important and worthy of attention (Prager et al., 2010).

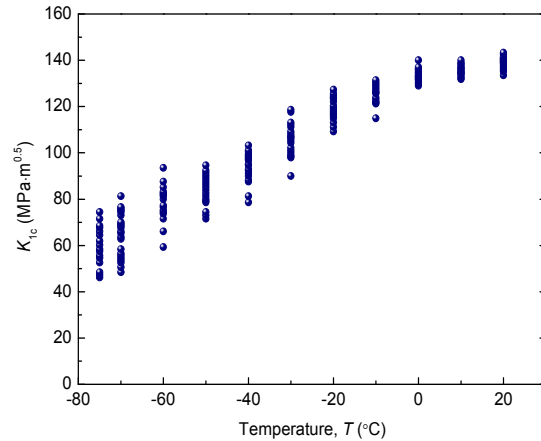


Fig. 8 Quasi-static fracture toughness as a function of the temperature based on the CVN tests

As recommended by API 579-1/ASME FFS-1 and WRC 528, the dynamic fracture toughness  $K_{I_d}$  with the loading rate of the CVN impact tests was chosen for generating the exemption curves. The  $K_{I_d}$  data were obtained based on the fact that the  $K_{I_d}$ – $T$  curve has a shape very similar to that of the  $K_{Ic}$ – $T$  curve in the transition region. A temperature-shift method was used by introducing a constant temperature offset  $\Delta T_s$ :

$$K_{1d}(T) = K_{1c}(T - \Delta T_S). \quad (18)$$

In this study,  $\Delta T_S$  was 41.67 K, as suggested in WRC 528, with the loading rate changing from quasi-static to the loading rate of the CVN impact test and would cover most cases influenced by loading rates (Barsom, 1975; Marandet and Sanz, 1977; ASME, 2007; Prager et al., 2010).

### 3.2.3 Curve fitting of $K_{1d}$

The fracture toughness data at multiple temperatures can be fitted by a hyperbolic tangent equation developed by the Materials Properties Council (Prager et al., 2010), as shown in Eq. (19):

$$K_{1d} = \frac{A_1 + A_2}{2} + \frac{A_1 - A_2}{2} \tanh\left(\frac{T - A_3}{A_4}\right), \quad (19)$$

where  $A_i$  ( $i=1, 2, 3, 4$ ) are four coefficients that describe the  $K_{1d}-T$  curve.  $A_1$  represents the upper shelf value,  $A_2$  is for the lower shelf value.  $A_3$  indicates a reference temperature corresponding to the mean value of the upper shelf and lower shelf fracture toughness. In the ASME code, four exemption curves (A, B, C, and D) correspond to four reference temperatures, 45.56 °C, 24.44 °C, 3.33 °C, and -11.11 °C, respectively.  $A_4$  is the half-width of the transition region.

To perform the fitting, the lower shelf value of fracture toughness was set to 17.57  $\text{MPa}\sqrt{\text{m}}$ , which corresponds to a CVN energy of 1.46 J measured at -196 °C. Thus,  $A_2$  equals 17.57 in Eq. (19). Then  $A_1$ ,  $A_3$ , and  $A_4$  were fitted based on the  $K_{1d}-T$  data, resulting in

$$K_{1d,\text{fit}} = 85.15 + 67.58 \tanh\left(\frac{T + 8.85}{61.14}\right). \quad (20)$$

The fitted curve of the dynamic fracture toughness as a function of the temperature given by Eq. (20) is plotted in Fig. 9, with the corresponding experimental scatter. The upper shelf value of fracture toughness is 152.73  $\text{MPa}\sqrt{\text{m}}$ , and the corresponding reference temperature is -8.85 °C. Regression analysis was carried out with respect to the 95% prediction intervals (Fig. 9).

The dynamic fracture toughness of a worst-case scenario  $K_{1d,\text{wcs}}$  was approximately estimated by using a temperature-shift method based on the fitted correlation Eq. (20). The point *A* on the fitted dynamic fracture toughness curve ( $K_{1d,\text{fit}}$ ) with the reference temperature of -8.85 °C was projected onto the lower prediction limit,  $K_{1d,95\%,\text{LPL}}$  curve, along the vertical direction to obtain a low-boundary reference point *B* (-8.85 °C and 73.42  $\text{MPa}\sqrt{\text{m}}$ ) (Fig. 9). Then the temperature offset  $\Delta T_P$  of 10.73 K between point *B* and the  $K_{1d,\text{fit}}$  curve was measured. Finally, the  $K_{1d,\text{fit}}$  curve was right-shifted by  $\Delta T_P$  to obtain the  $K_{1d,\text{wcs}}$  curve, shown as the dashed line in Fig. 9. Thus,

$$\begin{aligned} K_{1d,\text{wcs}}(T) &= K_{1d,\text{fit}}(T - \Delta T_P) \\ &= 85.15 + 67.58 \tanh\left(\frac{T - 1.88}{61.14}\right), \end{aligned} \quad (21)$$

resulting in a corresponding reference temperature of 1.88 °C. From a reliability and safety point of view,  $K_{1d,\text{wcs}}$  was finally taken into the calculation for the exemption curve for Q345R.

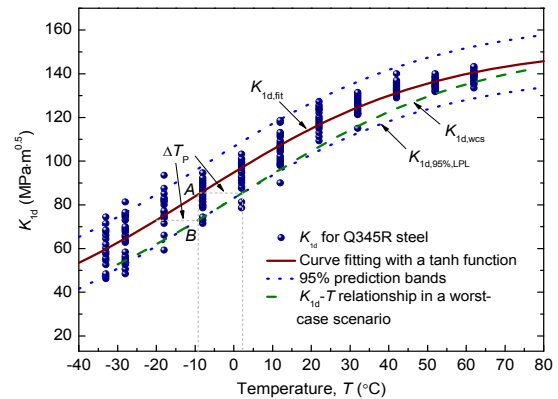


Fig. 9 Fitted dynamic fracture toughness curve for Q345R steel with the corresponding experimental scatter

### 3.3 Exemption curves

Impact test exemption curves are generated based on the requirement that the fracture toughness of the material shall be greater than the minimum permitted fracture toughness, as

$$K_c(T) \geq K_{1(\text{min})}(t). \quad (22)$$

The MDMT is defined as the temperature at which the fracture toughness equals the minimum permitted value:

$$K_c(\text{MDMT}) = K_{I(\min)}(t). \quad (23)$$

By substituting Eq. (21), in which  $K_{I_{d,wcs}}$  with a 95% lower prediction bound stands conservatively for the fracture toughness of the material, into Eq. (23) and rearranging, the MDMT is given by

$$\text{MDMT}(t) = \begin{cases} 61.14 \times \operatorname{artanh} \left[ \frac{K_{I(\min)}(t) - 85.15}{67.58} \right] + 1.88, & t \geq 10 \text{ and } \text{MDMT} \geq -50, \\ \text{MDMT}(10) \text{ or } -50, & t < 10 \text{ or } \text{MDMT} < -50. \end{cases} \quad (24)$$

Here, from a reliability and safety point of view, the cut-off limit for the lower bound of the curve was taken as  $-50^\circ\text{C}$  or the temperature at which the thickness was 10 mm, as assumed in WRC 528. The final resultant exemption curves are plotted in Fig. 10.

## 4 Discussion

### 4.1 Comparison with the ASME exemption curves

The exemption curve for Q345R is not in parallel to the ASME curve (Fig. 10). Its plateau corresponding to the thin components is located between the ASME curves C and D. Also, it rises more rapidly as the component thickness increases, and intersects the ASME curve C at  $(-7^\circ\text{C}/23\text{ mm})$  for AW and at  $(-7^\circ\text{C}/59\text{ mm})$  for PWHT/NW.

Such differences between the specific exemption curve of Q345R and the universal exemption curves of ASME are explained as follows.

A yield strength of 351 MPa was measured for Q345R and selected for calculating  $K_{I(\min)}$ , whereas the ASME exemption curves use 551.6 MPa for identifying all materials. A small  $\sigma_{ys}$  reduces the minimum required fracture toughness of the material and its sensitivity to the component thickness (Fig. 11a). Given the same component thickness range, the toughness range of interest for generating

the exemption curve is reduced to 50–98  $\text{MPa}\sqrt{\text{m}}$  (for AW) and 31–98  $\text{MPa}\sqrt{\text{m}}$  (for PWHT/NW), compared with 79–154  $\text{MPa}\sqrt{\text{m}}$  (for AW) and 49–154  $\text{MPa}\sqrt{\text{m}}$  (for PWHT/NW) for the ASME curves. The hyperbolic tangent correlation according to MPC is used to identify the dynamic fracture toughness of the materials as a function of the temperature. However, the  $K_{I_d}-T$  curve for Q345R is very different from the ASME references (Fig. 11b). Table 2 shows the correlation coefficients for both the ASME references and Q345R.

The upper shelf ( $A_1$ ) and lower shelf ( $A_2$ ) values for Q345R are both reduced significantly compared with the ASME references. Consequently, the  $K_{I_d}-T$  curve for Q345R is greatly compressed. In contrast, the transition range width ( $A_4$ ) of Q345R is 66.7%

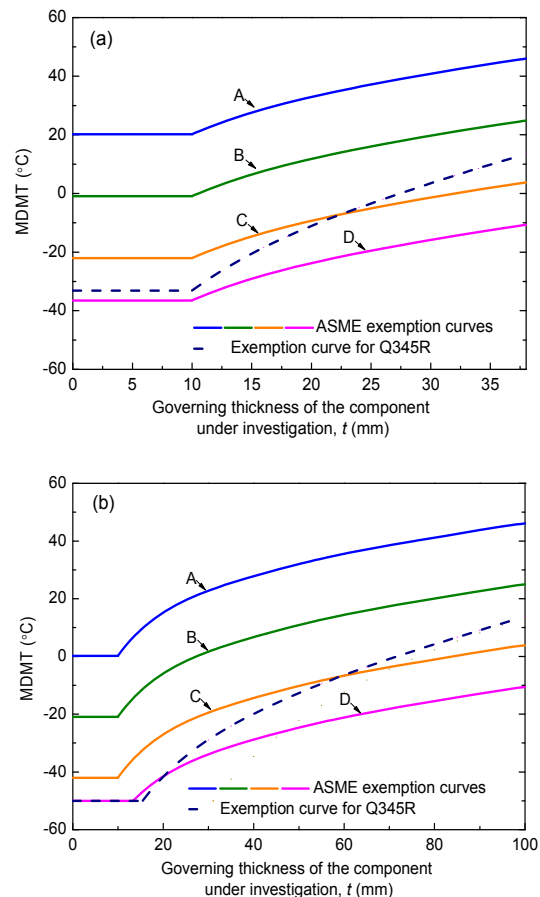


**Fig. 10 Exemption curves for Q345R compared with those of ASME**

(a) Under as-welded conditions; (b) Under post-weld heat treatment (PWHT) or non-welded (NW) conditions

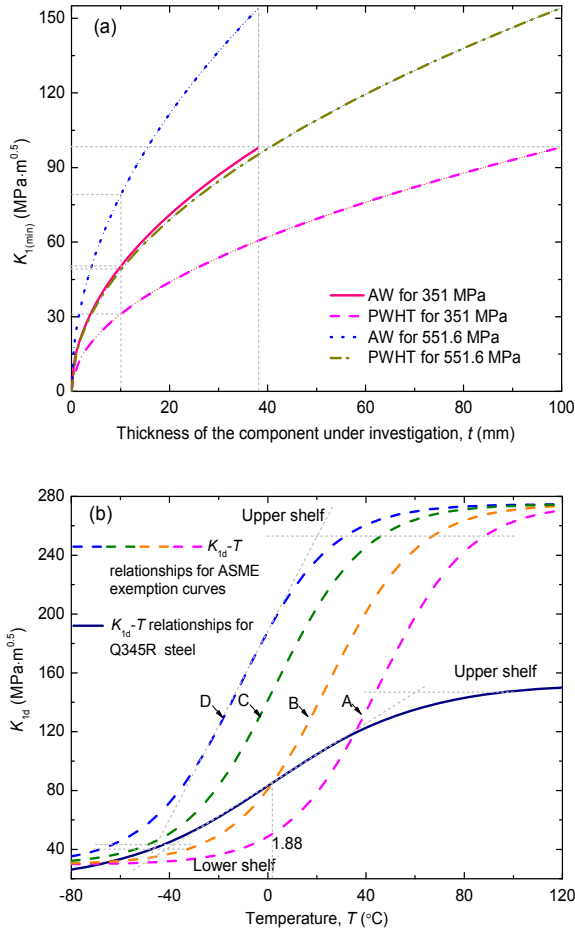


**Fig. 11 Comparisons between Q345R steel with  $\sigma_{ys}$  of 351 MPa and the ASME code for all materials with  $\sigma_{ys}$  of 551.6 MPa**  
 (a)  $K_{I(\min)}$ - $t$  relationships for both under as-welded condition (AW) and post-weld heat treatment (PWHT) or non-welded (NW) conditions; (b) Experimental  $K_{I,d}$ - $T$  relationship for Q345R steel and the  $K_{I,d}$ - $T$  relationships for ASME exemption curves

larger than that of the ASME references, resulting in a  $K_{I,d}$ - $T$  curve stretching in the horizontal direction (Fig. 11b). As a result, within the toughness range of interest, the fracture toughness is less sensitive to the temperature. Therefore, the steeper exemption curve of Q345R can be explained by the fact that, compared with the ASME references, the sensitivity of the fracture toughness to temperature is reduced more than the sensitivity to the component thickness.

Furthermore, the vertical position of the Q345R exemption curve is proved by its reference temperature of 1.88 °C, which is slightly less than that of ASME Group C. Combining the actual Q345R curve,

it is safe to classify Q345R into ASME Group B instead of Group A. Based on this more accurate method, we recommend that rather than using the ASME exemption curve, the specific exemption curve of Q345R should be used for determining whether an impact test is needed for a given Q345R component operating at a certain temperature. Such a specific curve expands the impact test exemption area, especially for small components with a thickness of less than 20 mm, and greatly simplifies the design process.

**Table 2 Coefficients of the MPC hyperbolic tangent correlation relating the dynamic fracture toughness to the temperature: ASME references vs. Q345R**

Item	$A_1$ (MPa·√m)	$A_2$ (MPa·√m)	$A_3$ (°C)	$A_4$ (°C)
ASME	A	274.81	29.67	45.46
	B	274.81	29.67	24.44
	C	274.81	29.67	3.33
	D	274.81	29.67	-11.11
Q345R	152.73	17.57	1.88	61.14

$A_1, A_2, A_3,$  and  $A_4$  are the coefficients of the MPC hyperbolic tangent correlation that describe the  $K_{I,d}$ - $T$  curve according to Eq. (19)

#### 4.2 Comparison with the master curve method

Besides the MPC method used in this study, the MC method is an alternative way to obtain the  $K_c$ - $T$  relationship. Based on the weakest-link theory (Wallin, 1984, 2007, 2010; Wallin et al., 2001; Taylor et al., 2006; Wallin and Laukkanen, 2008), the MC method has been widely used for estimating the probability distribution of the quasi-static fracture toughness of ferritic steels in recent years. After using the MC method and the fracture mechanics assessment procedure, Cui et al. (2015) discussed the applicability of the ASME exemption curve for Q345R and suggested that Q345R can be used at a temperature much lower than -10 °C and should be classified into ASME exemption curve D, which differs from the conclusion of this study for Q345-2009. However, in their study (Cui et al., 2015), the specified exemption curve for Q345R was not developed and the influence of the loading rate was not considered.

Considering the effect of different batches of Q345R, the MPC method and the MC method have been compared based on the  $K_{Ic}$  data (for the MPC

method) and the  $K_{Jc}$  data (for the MC method) from the same batch, Q345R-2014, for which the CVN test data and the fracture toughness test data are presented in Fig. 3 and Fig. 4b, respectively.

Therefore, as in Section 3.2, by using the conversion method described in Eqs. (13) and (14) and linear interpolation, the CVN data were empirically converted into  $K_{Jc}$  data versus the temperature. By applying the temperature shift method as presented in Eq. (18), the best fitted curve for the converted  $K_{1d}$  data is written as

$$K_{1d,fit,2014} = 130.47 + 112.90 \tanh\left(\frac{T + 39.68}{62.18}\right). \quad (25)$$

The temperature offset  $\Delta T_{p,2014}$  of 34.31 K was also introduced to estimate the dynamic fracture toughness  $K_{1d,wcs,2014}$  in a worst-case scenario. Thus,

$$\begin{aligned} K_{1d,wcs,2014}(T) &= K_{1d,fit,2014}(T - \Delta T_{p,2014}) \\ &= 130.47 + 112.90 \tanh\left(\frac{T + 5.37}{62.18}\right). \end{aligned} \quad (26)$$

Similarly, the expression for fracture toughness using the MC method (Fig. 4b) can be modified as

$$\begin{aligned} K_{Jc(0.05)} &= 20 + \left[ \ln\left(\frac{1}{1 - 0.05}\right) \right]^{0.25} \\ &\times \{11 + 77 \exp[0.019(T + 104.52)]\}. \end{aligned} \quad (27)$$

This expression describes the 5% tolerance bound of the mean  $K_{Jc}$  curve for the MC method with the same specimen thickness of 1T (25.4 mm) for the MPC method, and varies with the temperature. In Eq. (27),  $K_{Jc}$  represents the quasi-static fracture toughness. By using the temperature-shift method, it is converted into the dynamic fracture toughness:

$$K_{1d,MC} = 20 + 0.48 \times \{11 + 77 \exp[0.019(T + 62.85)]\}. \quad (28)$$

The relationship between  $K_{1d}$  and  $T$  obtained from the MPC method (Eq. (26)) and the MC method (Eq. (28)) is plotted in Fig. 12). The  $K_{1(\min)}$ , i.e.  $K_c$ (MDMT) (according to Eq. (23)), for Q345R-2014

with  $\sigma_{ys}$  of 408 MPa is generally less than  $114 \text{ MPa}\sqrt{\text{m}}$  (Fig. 13).

The thickness cut-off limit for calculating the MDMT of 10 mm corresponded to  $58 \text{ MPa}\sqrt{\text{m}}$  for AW and  $36 \text{ MPa}\sqrt{\text{m}}$  for PWHT/NW. Furthermore, the temperature cut-off limit for calculating MDMT was  $-50 \text{ }^\circ\text{C}$ . Therefore, a zone of interest can be drawn for the exemption curve generation (Fig. 12). In this zone,  $K_{1d}$  from the MPC method lies below that from the MC method, confirming that the MC method gives a higher evaluation on toughness for Q345R-2014 than that from the MPC method.

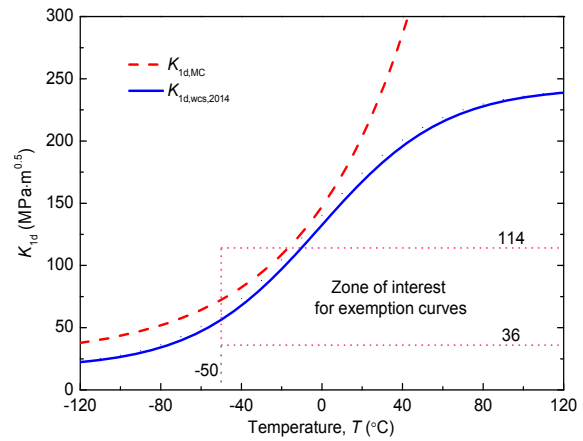


Fig. 12  $K_{1d}$ - $T$  relationships for Q345R-2014

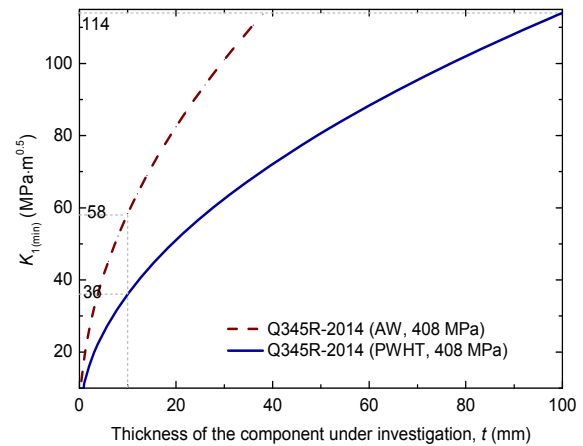
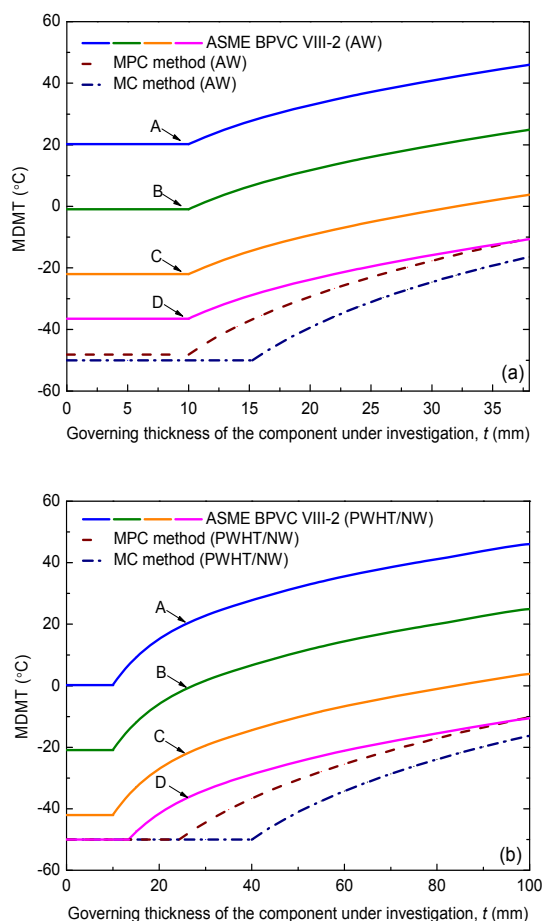


Fig. 13  $K_{1(\min)}$ - $t$  relationships for Q345R-2014

The exemption curves for Q345R-2014 based on the MPC method and the MC method are presented along with the ASME exemption curves in Fig. 14a and Fig. 14b for AW and PWHT/NW, respectively.

For both AW and PWHT/NW, the exemption curve generated from the MPC method lies below the ASME exemption curve D, confirming that this Q345R meets the requirements of the curve D. According to the MC method, Group D is also suitable for this Q345R, of which the exemption curve has a similar shape with, but lies even below that from the MPC method. Based on a rigorous theoretical basis in statistics, the exemption curve for Q345R-2014 from the MC method is reliable. Thus, it can be concluded that both exemption curves from the MC method and the MPC method for Q345R-2014 are reliable, and the MC method expands a further area for the impact test exemption and results in a lower MDMT for Q345R steel than the MPC method.



**Fig. 14 Comparisons among the ASME exemption curves and exemption curves for the same Q345R-2014 based on the MPC method and the MC method**

(a) As-welded condition (AW); (b) Post-weld heat treatment or non-welded condition (PWHT/NW)

## 5 Conclusions

In this paper, specific exemption curves under AW and PWHT/NW conditions are presented based on the FAD approach and extensive CVN tests for both Q345R-2009 and Q345R-2014. To determine the empirical relationship between CVN energies and quasi-static fracture toughness data for Q345R steel, the Sailors–Corten correlation proved to be more accurate and suitable based on test data and the MC method. The specific exemption curve for Q345R-2009 was not in parallel to the ASME curves and lay over curve C and between curves B and D. The specific exemption curves for Q345R-2014 lay below curve D. It is safe to classify Q345R into ASME Group B instead of Group A by reference to the mechanical properties of the worst batch of Q345R steel, Q345R-2009. With a more accurate method, we suggest using the specific exemption curve of Q345R for determining whether an impact test is needed for a given Q345R component operating at a certain temperature. Such a specific curve expands the impact test exemption area, especially for small components with a thickness of less than 20 mm, and greatly simplifies the design process. The method presented in this paper (MPC method) was compared to the MC method. We concluded that both the two methods are reliable for determining the exemption curve for certain materials, and the MC method expands a further area for the impact test exemption and results in a lower MDMT than the MPC method.

## References

- ASME (American Society of Mechanical Engineers), 2007. Fitness-for-Service, 2nd Edition, API 579-1/ASME FFS-1:2007. The American Petroleum Institute, Washington DC, USA.
- ASME (American Society of Mechanical Engineers), 2010. Boiler and Pressure Vessel Code Case, B&PV Code Case 2642:2010. ASTM International, New York, USA.
- ASME (American Society of Mechanical Engineers), 2015a. Boiler and Pressure Vessel Code Section VIII Division 1: Rules for Construction of Pressure Vessels, BPVC VIII-1:2015. ASTM International, New York, USA.
- ASME (American Society of Mechanical Engineers), 2015b. ASME Boiler and Pressure Vessel Code Section VIII Division 2: Alternative Rules Rules for Construction of Pressure Vessels, BPVC VIII-2:2015. ASTM International, New York, USA.

- ASTM (American Society for Testing and Materials), 2012. Standard Test Method for Linear-Elastic Plane-Strain Fracture Toughness  $K_{Ic}$  of Metallic Materials, E399-12e3:2012. ASTM International, West Conshohocken, USA.
- ASTM (American Society for Testing and Materials), 2016. Standard Test Method for Determination of Reference Temperature,  $T_0$ , for Ferritic Steels in the Transition Range, E1921:2016. ASTM International, West Conshohocken, USA.
- Barsom JM, 1975. Development of the AASHTO fracture-toughness requirements for bridge steels. *Engineering Fracture Mechanics*, 7(3):605-618.  
[https://doi.org/10.1016/0013-7944\(75\)90060-0](https://doi.org/10.1016/0013-7944(75)90060-0).
- Barsom JM, Rolfe ST, 1970. Correlations between  $K_{Ic}$  and Charpy V-notch test results in the transition-temperature range. In: Driscoll DE (Ed.), ASTM STP 466 Impact Testing of Metals. ASTM International, West Conshohocken, USA, p.281-302.  
<https://doi.org/10.1520/STP32067S>
- BSI (British Standard Institution), 2005. Guide to Methods for Assessing the Acceptability of Flaws in Metallic Structures, BS 7910:2005. British Standard Institution, London, UK.
- Cao Y, Hui H, Xuan F, 2008. Study on fracture toughness of 16MnR steel in the transition-temperature region using the master curve method. *Pressure Vessel Technology*, 25(12):10-21 (in Chinese).  
<https://doi.org/10.3969/j.issn.1001-4837.2008.12.003>
- Cui Q, Hui H, Li P, 2015. Applicability of the ASME exemption curve for Chinese pressure vessel steel Q345R. *Journal of Pressure Vessel Technology*, 137(6):061602.  
<https://doi.org/10.1115/1.4030673>
- Gui L, Shou B, Xiu T, 2016. Estimation of Q345R fracture toughness based on master curve. *Pressure Vessel Technology*, 33(2):10-16 (in Chinese).  
<https://doi.org/10.3969/j.issn.1001-4837.2016.02.002>
- Marandet B, Sanz G, 1977. Evaluation of the toughness of thick medium-strength steels by using linear elastic fracture mechanics and correlations between  $K_{Ic}$  and Charpy V-Notch. *ASTM Special Technical Publication*, 631:72-95.  
<https://doi.org/10.1520/STP35533S>.
- Prager M, Osage DA, Staats J, 2010. Development of Material Fracture Toughness Rules for the ASME B&PV Code, Section VIII, Division 2, Welding Research Council Bulletin 528. The Welding Research Council, New York, USA.
- PVRC (Pressure Vessel Research Committee), 1972. PVRC Recommendations on Toughness Requirements for Ferritic Materials, Welding Research Council Bulletin 175. The Welding Research Council, New York, USA.
- Roberts R, Newton C, 1981. Interpretive Report on Small-scale Test Correlations with  $K_{Ic}$  Data, Welding Research Council Bulletin 265. The Welding Research Council, New York, USA.
- Rolfe ST, Novak SR, 1970. Slow-bend  $K_{Ic}$  testing of medium-strength high-toughness steels. In: Brown W (Ed.), ASTM STP 463 Review of Development in Plane Strain Fracture Toughness Testing. ASTM International, West Conshohocken, USA, p.124-159.  
<https://doi.org/10.1520/STP33665S>
- SAC (Standardization Administration of the People's Republic of China), 1998. Steel and Steel Product: Location and Preparation of Test Pieces for Mechanical Testing, GB/T 2975:1998. SAC, Beijing, China (in Chinese).
- SAC (Standardization Administration of the People's Republic of China), 2014. Steel Plates for Boilers and Pressure Vessels, GB/T 713:2014. SAC, Beijing, China (in Chinese).
- Sailors RH, Corten HT, 1971. Relationship between material fracture toughness using fracture mechanics and transition temperature tests. In: Corten H (Ed.), ASTM STP 514 Fracture Toughness: Part II. ASTM International, West Conshohocken, USA, p.164-191.
- Shu X, Zheng J, Shou B, 2013. Experimental investigation on minimum design metal temperature of Q345R steel. In: Pressure Vessels and Piping Division. American Society of Mechanical Engineers, Paris, France.  
<https://doi.org/10.1115/PVP2013-97763>
- Taylor N, Minnebo P, Siegle D, et al., 2006. Use of master curve technology for assessing shallow flaws in a reactor pressure vessel material. In: Pressure Vessels and Piping Division. American Society of Mechanical Engineers, Vancouver, Canada.  
<https://doi.org/10.1115/PVP2006-ICPVT-11-93640>
- Thorby PN, Ferguson WG, 1976. Fracture toughness of HY60. *Materials Science and Engineering*, 22(2):177-184.  
[https://doi.org/10.1016/0025-5416\(76\)90151-8](https://doi.org/10.1016/0025-5416(76)90151-8)
- Wallin K, 1984. The scatter in  $K_{Ic}$ -results. *Engineering Fracture Mechanics*, 19(6):1085-1093.  
[https://doi.org/10.1016/0013-7944\(84\)90153-X](https://doi.org/10.1016/0013-7944(84)90153-X)
- Wallin K, 2007. Use of the master curve methodology for real three dimensional cracks. *Nuclear Engineering and Design*, 237(12-13):1388-1394.  
<https://doi.org/10.1016/j.nucengdes.2006.09.034>
- Wallin K, 2010. Structural integrity assessment aspects of the master curve methodology. *Engineering Fracture Mechanics*, 77(2):285-292.  
<https://doi.org/10.1016/j.engfracmech.2009.02.010>
- Wallin K, Laukkanen A, 2008. New developments of the Wallin, Saario, Torronen cleavage fracture model. *Engineering Fracture Mechanics*, 75(11):3367-3377.  
<https://doi.org/10.1016/j.engfracmech.2007.07.018>
- Wallin K, Rintamaa R, Nagel G, 2001. Conservatism of ASME KIR-reference curve with respect to crack arrest. *Nuclear Engineering and Design*, 206(2-3):185-199.  
[https://doi.org/10.1016/S0029-5493\(00\)00434-9](https://doi.org/10.1016/S0029-5493(00)00434-9)

## 中文概要

**题目:** Q345R 钢最低设计金属温度的试验研究

**目的:** Q345R 是中国应用最多、最广泛的压力容器钢板材料,其低温韧性在国际上被严重低估。本文旨在通过大量试验研究,探明 Q345R 在低温下的实际韧性表征,得到其特有的冲击试验豁免曲线,并确定其合适的使用温度范围。

**创新点:** 1. 基于大量低温试验数据,并考虑应变率的影响,得到了 Q345R 特有的冲击试验豁免曲线; 2. 采用主曲线方法代替纯冲击试验方法评价 Q345R 低温韧性,得到了基于主曲线方法的 Q345R 豁免曲线; 3. 通过比较两类韧性评价方法所得的豁免曲线,最终确定合适的 Q345R 使用温度范围。

**方法:** 1. 利用试验获得大量的冲击试验数据(图 3),通过计算  $K_{I(\min)}-t$  关系(图 5)和  $K_c-T$  关系(图 9),并考虑应变率的影响(公式(18)),得到 Q345R 特有的冲击试验豁免曲线(图 10); 2. 利用试验方法获得 Q345R 的主曲线(图 4),并用其代替原来的  $K_c-T$  关系,得到基于主曲线方法的 Q345R 豁免曲线(图 14); 3. 比较两类方法的  $K_{I_d}-T$  关系(图 13)和豁免曲线(图 14)。

**结论:** 1. Q345R 的低温韧性在国际上被严重低估; 2. 得到了 Q345R 特有的冲击试验豁免曲线及其合适的使用温度范围; 3. 主曲线方法的引入能进一步拓展 Q345R 的使用温度范围。

**关键词:** Q345R; 低温韧性; 冲击试验豁免曲线; 使用温度; 主曲线